✤ *Author's Choice*

Characterization of a novel HMG-CoA lyase enzyme with a dual location in endoplasmic reticulum and cytosol[S]

María Arnedo,* Sebastián Menao,* Beatriz Puisac,* María E. Teresa-Rodrigo,* María C. Gil-Rodríguez,* Eduardo López-Viñas,[†,§] Paulino Gómez-Puertas,[†] Nuria Casals, César H. Casale,[††] Fausto G. Hegardt,[§§] and Juan Pié[1,*]**

Unit of Clinical Genetics and Functional Genomics,* Department of Pharmacology and Physiology, School of Medicine, University of Zaragoza, Spain; Molecular Modeling Group,[†] Centro de Biología Molecular "Severo Ochoa" (CSIC-UAM), Madrid, Spain; Biomol-Informatics SL,[§] Parque Científico de Madrid, Spain; Basic Sciences Department,** Universitat Internacional de Catalunya, Catalunya, Spain; Department of Molecular Biology,[††] National University of Río Cuarto, Río Cuarto, Argentina; and Department of Biochemistry,[§§] School of Pharmacy, University of Barcelona, Barcelona, Spain

Abstract **A novel lyase activity enzyme is characterized for the first time: HMG-CoA lyase-like1 (er-cHL), which is a close homolog of mitochondrial HMG-CoA lyase (mHL). Initial data show that there are nine mature transcripts for the novel gene *HMGCLL1*, although none of them has all its exons. The most abundant transcript is called "variant b," and it lacks exons 2 and 3. Moreover, a three-dimensional model of the novel enzyme is proposed. Colocalization studies show a dual location of the er-cHL in the endoplasmic reticulum (ER) and cytosol, but not in mitochondria or peroxisomes. Furthermore, the dissociation experiment suggests that it is a nonendoplasmic reticulum integral membrane protein. The kinetic parameters of er-cHL indicate that it has a lower V_{max} and a higher substrate affinity than mHL. Protein expression and lyase activity were found in several tissues, and were particularly strong in lung and kidney. The occurrence of er-cHL in brain is surprising, as mHL has not been found there. Although mHL activity is clearly associated with energy metabolism, the results suggest that er-cHL is more closely related to another metabolic function, mostly at the pulmonary and brain level.**—Arnedo, M., S. Menao, B. Puisac, M. E. Teresa-Rodrigo, M. C. Gil-Rodríguez, E. López-Viñas, P. Gómez-Puertas, N. Casals, C. H. Casale, F. G. Hegardt, and J. Pié. **Characterization of a novel HMG-CoA lyase enzyme with a dual location in endoplasmic reticulum and cytosol. *J. Lipid Res.* 2012.** 53: **2046–2056.**

Supplementary key words enzymology • kinetics • liver • lung • brain • ketone bodies • lyase activity • endoplasmic reticulum-cytosolic HMG-CoA lyase • mitochondrial HMG-CoA lyase

The 3-hydroxy-3-methylglutaryl CoA lyase, or human HMG-CoA lyase (HL), catalyzes the cleavage of 3-hydroxy-3-methylglutaryl CoA (HMG-CoA) to acetoacetate and acetyl-CoA. This reaction is the common final step in ketogenesis and leucine catabolism (1). There are two isoforms of the HL protein, one mitochondrial and the other peroxisomal (2). Both exhibit lyase activity and are encoded by the same gene: *HMGCL*. The HL enzyme has been crystallized (3, 4), and the most critical residues for catalytic function, Arg^{41}, Glu^{72}, Tyr^{167} and Cys^{266}, are known. Moreover, the residues that bind to the divalent cation Mg^{2+}, which are essential for lyase activity (Asp^{42}, Asn^{275}, His^{233}, and His^{235}), are also known (3–9).

The mitochondrial isoform contributes to ketone body production, and it has been studied in depth. It has a homodimer TIM-barrel structure, joined by di-sulfur bridges (2, 3, 6, 10). It is mainly expressed in liver, a ketogenic tissue, but expression and activity levels have been reported in other human tissues, such as pancreas, kidney, and skeletal muscle (11). Its failure causes HL deficiency or 3-hydroxy-3-methylglutaric aciduria (MIM 246450), a rare autosomal recessive disease that appears with hypoglycemic states and is accompanied by hypoketosis and metabolic acidosis (1, 12, 13).

The function of the peroxisomal isoform is still unknown (2). It has been proposed that it could play a role

This study was supported by grants from the Diputación General de Aragón (DGA) (Grupo Consolidado B20 and PI1 28/08), European Social Fund ("Construyendo Europa desde Aragón"), the University of Zaragoza (Ref. # UZ2009-BIO-04 and # PIF-UZ_2009-BIO-02), and the Spanish Ministerio de Economía y Competitividad (MINECO) (Grant SAF2011-30520-C02-02).

✤ ***Author's Choice**—Final version full access.*

Manuscript received 21 February 2012 and in revised form 12 July 2012.

Published, JLR Papers in Press, July 30, 2012
DOI 10.1194/jlr.M025700

Abbreviations: 3HG, 3-hydroxy-glutaric acid; 3D, three-dimensional; EGFP, enhanced green fluoresce protein; ER, endoplasmic reticulum; er-cHL, 3-hydroxy-3-methylglutaryl coenzyme A lyase like 1; EST, expressed sequence tag; HL, 3-hydroxy-3-methylglutaryl coenzyme A lyase; mHL, mitochondrial 3-hydroxy-3-methylglutaryl coenzyme A lyase; MBP, maltose binding protein; PDB, protein data bank; pHL, peroxisomal 3-methylglutaryl coenzyme A lyase; PNS, post-nuclear supernatant; WT, wild type.

[1] To whom correspondence should be addressed.
e-mail: juanpie@unizar.es

[S] The online version of this article (available at http://www.jlr.org) contains supplementary data in the form of three figures.

in cholesterol synthesis (2) or in long-chain fatty acid degradation (14). Entry to the peroxisomes is due to the CKL signal tripeptide of the C-terminal end. The peroxisomal isoform is 2.5 kDa larger than the mitochondrial isoform because of the presence in the structure of the mitochondrial signal peptide (2). Initially, the peroxisomal isoform was thought to be monomeric (15), but it was subsequently identified as a homodimer (16). Despite the differences in size and amino acid sequence between the two isoforms, their kinetic activity values of K_m and kcat are close (15).

In this article we report, for first time, the finding of another HL isoenzyme, 3-hydroxy-3-methylglutaryl CoA lyase-like 1 (er-cHL, Uniprot code: Q8TB92, HMGC2_HUMAN), encoded by a different gene: *HMGCLL1*. Our initial studies show that er-cHL is located in the endoplasmic reticulum (ER) and the cytosol of cell cultures. We show that er-cHL has a structural homology with mHL protein, but it has a differential tissue expression pattern and distinct kinetic parameters. These findings suggest that the novel er-cHL isoform has a different function than mHL, which may be to synthesize ketone bodies in the cytosol.

EXPERIMENTAL PROCEDURES

Samples

Tissue samples of brain, pancreas, liver, testis, lung, and kidney were obtained from adult humans within 24 h post mortem in the Department of Pathology at the University of Zaragoza. Representative samples of organs of approximately 1–2 g were taken from each subject. The bodies were kept at 4°C until autopsy, and all the tissues obtained were immediately deep-frozen in N_2 and stored at −80°C until use. These actions minimized the protein degradation of the samples.

For the splicing variants, Multiple Tissue cDNA (MTC) panels (Clontech) from adult and fetal tissues were used as samples.

Cell culture

Human embryonic kidney fibroblast 293 (HEK293) were grown on lysine-treated coverslips in 24-well or in 10 cm plates to 70–80% confluence in DMEM (Dulbecco's Modified Eagle's Medium; Sigma) supplemented with 10% fetal calf serum (Sigma), penicillin (100 units/ml), streptomycin (100 μg/ml), and L-glutamine 2 mM in a 5% CO_2 atmosphere.

Bioinformatics databases

The following bioinformatics databases were used in this study: the National Center for Biotechnical Information (Gene database) (http://www.ncbi.nlm.nih.gov/gene/), Ensembl (http://www.ensembl.org), UniProt (http://www.uniprot.org/), and UniGene (http://www.ncbi.nlm.nih.gov/unigene). The Splice Site Prediction (http://www.fruitfly.org/seq_tools/splice.html) algorithm was used to calculate the strength of splice sites.

Overlapping fragment analysis of splice variants

An exhaustive analysis of the *HMGCLL1* mRNA transcripts was performed using 12 primers that produced 12 overlapping fragments. We explored *HMGCLL1* transcript variants in cDNA from brain, lung, kidney, liver, skeletal muscle, heart, and spleen of adult and fetal tissues using Multiple Tissue cDNA (MTC) panels (Clontech). The identity of all PCR products was confirmed by DNA sequencing using ABI Prism BigDye Terminator Cycle Sequencing v2.0 (Applied Biosystems), and the products were analyzed on an Applied Biosystems 5700 DNA sequencer.

Structural analysis and modeling procedures for human er-cHL protein

A 3D model of the protein core (residues 43–340) of human er-cHL (Uniprot code: Q8TB92, HMGC2_HUMAN) was generated using homology modeling procedures with Biomol-Informatics (http://www.biomol-informatics.com) software facilities. The coordinates of human mHL protein were used as a template [Protein Data Bank code: 2CW6 (3), blast value: 1.1×10^{-116}, sequence identity: 70%]. The model was built using the SWISS-MODEL server (17–19), which is available at <http://swissmodel.expasy.org//SWISS-MODEL.html>, and the structural quality was checked using the analysis programs provided by the same server (Anolea/Gromos). The overall model quality estimation score QMEAN4 (20) was 0.671. This score is within the range of scores accepted for homology-based structure models. To optimize the geometries, the model was energy minimized using the GROMOS 43B1 force field, implemented in DeepView (21) using 500 steps of the steepest descent minimization followed by 500 steps of conjugate-gradient minimization.

Plasmid constructions

To prepare constructs of *HMGCLL1*-pMAL-c2× and *HMGCL*-pMAL-c2×, we followed the protocol described by Menao et al. (2009) (22). cDNA was obtained from a lung cDNA library [Multiple Tissue cDNA (MTC) panels, Clontech]. The pMAL-c2× vector (Biolabs) was used to clone the coding region of *HMGCLL1* or *HMGCL*, except for the leader peptide sequence. Thus, we created recombinant plasmids in which the encoded er-cHL and mHL proteins were fused to the N-terminal region of maltose binding protein (MBP). These constructs enabled us to obtain a sufficient quantity of the er-cHL and mHL proteins in a prokaryotic model.

To prepare constructs of *HMGCLL1*-EGFP and *HMGCL*-Red, the pEGFP-N3 and pDsRed2-N1 vectors (Clontech) were used to clone the coding region of er-cHL (340 amino acids) or mHL (325 amino acids). er-cHL and mHL proteins were fused to the N-terminal region of EGFP and Red2 proteins, respectively. These constructs enabled us to localize the er-cHL and mHL proteins inside a eukaryotic cell.

To prepare constructs of *HMGCLL1*-Tag3 and *HMGCL*–Tag3, the pCMV-3Tag-3 vector (Agilent Technologies) was used to clone the coding region of er-cHL (340 amino acids) or mHL (325 amino acids). er-cHL and mHL proteins were fused to c-Myc epitope tag. These constructs enabled us to localize the er-cHL and mHL proteins inside a eukaryotic cell.

To prepare constructs of *HMGCLL1*-pIRES2, the vector pIRES2-EGFP vector (Clontech) was used. The coding region of human *HMGCLL1* was cloned into vector pIRES2-EGFP, which allowed both the gene of interest and the EGFP gene to be translated from a single bicistronic mRNA. This construct enabled us to overexpress the er-cHL protein in a eukaryotic model.

Directed mutagenesis

Mutants were generated using PCR according to Stratagene's QuickChange site-directed mutagenesis protocol. The *HMGCLL1*-pMAL-c2× construct was used as a template for single mutations. We performed the following single amino acid mutations: R56Q, H248R, and L207S. Mutations p.R56Q, p.L207S, and p.H248R were paralogous with the changes p.R41Q, p.F192S, and p.H233R in the mHL protein that cause enzyme activity loss. Mutations were verified by DNA sequence analysis.

We generated an exon 6 deletion mutant of the *HMGCLL1 (HMGCLL1Δ6)* gene using *HMGCLL1*-pIRES2 and the *HMGCLL1*-pMAL-c2× vectors as a template.

Protein overexpression

The er-cHL protein (wild-type and mutants) in the pMAL-c2× vector was expressed in *E. coli*. We followed the same protocol as that described by Menao et al. (2009) (22).

The er-cHL (wild-type and mutant) proteins in the pIRES2 vector were expressed in HEK293 cells. The recombinant vectors *HMGCLL1*-pIRES2 and *HMGCL*-pIRES2 were transfected using METAFECTENE™ PRO (Biontex), according to the manufacturer's protocol. Cells were recovered by centrifugation at 1,000 *g* for 5 min at 4°C. They were then washed in 1.5 ml of PBS, and resuspended in 2 ml of lysis buffer (30 mM NaCl, 6 mM NaF, 1 mM EDTA, 3 mM $Na_2HPO_4.7H_2O$, 3 mM NaPPi, 4 mM HEPES, 100 µg/ml PMSF, 1.5% Triton X-100). Homogenates were centrifuged at 10,000 rpm for 10 min at 4°C. The supernatant was immediately used in the HMG-CoA lyase activity assay.

Western blot experiments

A specific er-cHL antibody was developed against the immunological sequence NH_2-SMGKFEEVVKSARHMN-COOH of the er-cHL, from Abyntek S.A. Antibody specificity was tested by an enzyme-linked immunosorbent assay and Western blot.

Generally, 50 µg of protein sample was subjected to SDS-PAGE electrophoresis. A 1:1000 dilution of anti-er-cHL (Abyntek) or anti-mHL (Abnova) was used as the primary antibody. The secondary antibody was used at 1:1000 dilution. The blots were developed with the Immobilon Western Chemiluminescent HRP Substrate (Millipore) kit. The images captured were processed using Adobe Photoshop 5.0.

Colocalization studies in culture cells

Cultured cells were grown on lysine-treated coverslips in 24-well plates. Colocalization studies were performed 72 h after transfection with plasmid containing er-cHL or mHL fused to the 5′-end of EGFP and Red2 protein, respectively, using METAFECTENE™ PRO (Biontex) according to the manufacturer's protocol. To visualize the ER, the commercial pDsRed2-ER (Clontech) plasmid was cotransfected with the *HMGCLL1*-pEGFP. Cells were washed twice in phosphate-buffered saline (PBS) and fixed with 4% paraformaldehyde in PBS for 15 min at room temperature. The coverslips with the fixed cells were mounted on glass slides with Mowiol for the microscope visualization.

To visualize the er-cHL and mHL proteins fused to the c-Myc tag, HEK293 cells transfected with the plasmid *HMGCLL1*-Tag3 and *HMGCL*-Tag3 were washed twice in PBS and fixed with 4% paraformaldehyde in PBS for 15 min at room temperature. Then, cells were permeabilized with 1% (w/v) of Triton X-100 in PBS with glycine 20 mM for 10 min at room temperature and then washed twice in PBS. Nonspecific antibody binding was blocked by incubation with 1% (w/v) BSA in PBS with glycine 20 mM for 20 min at room temperature. Cells were incubated with rabbit monoclonal antibody anti-myc (GenScrip) [1:300 in 1% (w/v) BSA/PBS/20 mM glycine/0.2% Triton X-100] for 1 h at 37°C. After being washed twice in PBS/20 mM glycine, cells were incubated with goat anti-rabbit Alexafluor 488 (Molecular Probes) [1:500 in 1% (w/v) BSA/PBS/20 mM glycine/0.2% Triton X-100] for 1 h at 37°C, and then washed twice in PBS. Coverslips were mounted on glass slides with Mowiol.

Colocalization studies against peroxisomes, endoplasmic reticulum, and cytosolic proteins were carried out at the same time in the same cells using the suitable primary antibodies [rabbit anti-PMP70 (Zymed), mouse anti-calnexin (Santa Cruz Biotechnologies), and mouse anti-GAPDH (Santa Cruz Biotechnologies)] and developed with goat anti-mouse Alexafluor 546 or goat anti-rabbit Alexafluor 546 (Molecular Probes). We performed these experiments in HEK293 cells transfected with the plasmid *HMGCLL1*-pEGFP and with *HMGCLL1*-Tag3 simultaneously.

Fluorescent staining patterns were visualized using a fluorescence microscope (Leica). The images captured were processed using Adobe Photoshop 5.0.

Study of association-disassociation to the endoplasmic reticulum

For the association assay, we treated samples (endoplasmic reticulum from lung tissue and the cloned er-cHL protein) with 1% Triton X-114 following the protocol described by Casale et al. (2001) (23). To obtain phase separation, the preparation was warmed to 37°C for 5 min and then centrifuged at 1,000 rpm for 3 min. The aqueous upper phase and lower detergent-rich phases were carefully separated. We kept both phases to analyze them by Western blot.

For the dissociation assay, we followed the protocol previously described by Callan et al. (2007) (24) with some modifications. We treated the samples with $NaHCO_3$ 100 mM pH 11.5. Then, we separated the sample into two phases for centrifugation at 100,000 *g* for 20 min at 4°C. We kept the supernatant fraction and resuspended the pellet fraction in PBS, then added 2 ml of acetone and centrifuged it at 1,000 rpm for 10 min. Finally, we performed Western blot assays of the supernatant and pellet samples and developed them against er-cHL and calnexin proteins. We performed the same experiment using PBS-Triton X-100 (1%) as a detergent control treatment.

Subcellular fractionation

The protocol described by Clinkenbeard et al. (1975) (25) was followed with some modifications. Several adult human tissues (liver, lung, kidney, brain, pancreas, testis, heart, and skeletal muscle) were washed with ice-cold homogenizing buffer containing 0.25 M sucrose, 5 mM $MgCl_2$, 1 mM DTT, 1 mM PMSF, and 10 mM Tris pH 7.2. All operations were conducted at 4°C. The tissues were disrupted by a manual homogenizer. We obtained two fractions: the pellet that contained the mitochondrial fraction, and the supernatant fraction that contained all the organelles except the nuclei, mitochondria, and peroxisomes.

We performed an extra centrifugation at 100,000 *g* for 1 h at 4°C. We obtained two fractions: the pellet was the endoplasmic reticulum, and the supernatant was the cytoplasm fraction.

We carried out a Western blot experiment with the obtained fractions (total lysate, postnuclear soluble, and pellet and supernatant of the 100,000 *g*) to ascertain the subcellular location of the er-cHL protein.

HMG-CoA enzyme assay

HMG-CoA lyase activity was measured by a simple spectrophotometric method that determines the amount of acetoacetate produced. We followed the protocol described by Wanders et al. (1988) (26).

RESULTS

HMGCLL1 gene structure and splicing variants

The *HMGCLL1* gene is located on chromosome 6p12.1 (Gene database, Ensembl database). It contains 11 exons ranging from 64 bp to 334 bp, and 10 introns of between

223 bp and 55,859 bp. The *HMGCLL1* gene spans more than 160 kbp, but the *HMGCL* gene spans only 24 kbp. This discrepancy is due to the difference in the size of some introns of the *HMGCLL1* gene (supplemental Fig. I). The databases contain several variants of this gene, none of which has all the exons in its sequence. "Variant b" was the first to be described in the databases, and expressed sequence tags (EST) from this variant are more frequent than others. For this reason, we chose "variant b" of the *HMGCLL1* gene as a reference for all the splicing variants found. This variant contains 9 exons and 8 introns, like the *HMGCL* gene.

There are two additional variants of the gene *HMGCLL1*: "variant a" and "variant c." These variants have exon insertions: exon 2 in "variant a" and exon 3 in "variant c." However, when we tried to amplify these variants, we were unable to obtain the whole cDNA from them (the primers hybridized in the 5′- and 3′-UTR region of both variants). Exons 2 and 3 are defined as strong by the Splice Site Prediction program (score > 0.9). However, "variant a" and "variant c" could only be amplified when we used specific primers that hybridized with exon 2 or 3 of the gene.

To identify alternative splice variants of the *HMGCLL1* gene, a search of database ESTs and overlapping amplifications was carried out. The ESTs database search showed seven alternative splicing variants of the gene (deletions of the exons 2 to 7, 5 to 8, 6, 6 and 7, 6 to 8, and 6 to 9). The overlapping amplifications were performed with *HMGCLL1* cDNA from fetal and adult tissues. PCR amplification, which explored the whole gene, showed several bands (supplemental Fig. II) that belong to some of the splicing variants of the gene (deletions of exons 2 to 7, 2 to 9, 6, 6 and 7, 6 to 8, and 6 to 9).

Structural model for human er-cHL protein

A 3D structural model was generated for human er-cHL protein. The structures of some closely related homolog proteins were already available in the Protein Data Bank (PDB) as crystallized structures, allowing the generation of a good quality model for the protein catalytic core (residues 42–340). The model was built according to the 3D structure of human mHL protein. Sequence alignment of the catalytic domain of both proteins showed a sequence identity of 70% (supplemental Fig. III), with the complete absence of sequence insertions or deletions. All residues shared the putative catalytic site. Due to the close homology, the structure of the model generated was almost identical to the template protein (PDB: 2CW6) (3): a $(\beta\alpha)_8$ barrel with shorts loops at the NH_2-terminal face and longer loops in the COOH-terminal face, where the substrate molecule is located (**Fig. 1A**).

We carried out site-directed mutagenesis in er-cHL (R56Q, H248R, and L207S; Fig. 1A) to reproduce some previously described mutations of the mHL protein that cause the complete loss of enzymatic activity [R41Q (27), H233R (28), and F192S (22)]. R56 and H248 are catalytic residues located in the active center of the protein. L207 is located in α helix 5 and is part of a hydrophobic cluster that maintains the local structure, which is also composed of F165, V183, V203, and I215 (Fig. 1B). A mutation of Leu to Ser would destabilize the neighborhood, resulting in the disorganization of the closely located active center. This is similar to the effect exhibited by the equivalent mutant F192S in mHL (22). We overexpressed the mutants (Fig. 1C) and carried out enzyme measurements. As in the case of mHL mutants, the aforementioned er-cHL mutants are completely inactive (**Table 1**).

er-cHL subcellular localization

er-cHL is localized in the endoplasmic reticulum and in the cytosol of cultured cells. To study the subcellular localization of native er-cHL, protein kidney human tissue was fractionated. Total tissue, postnuclear supernatant, ER membrane and cytosol fractions (50 μg) were analyzed by Western

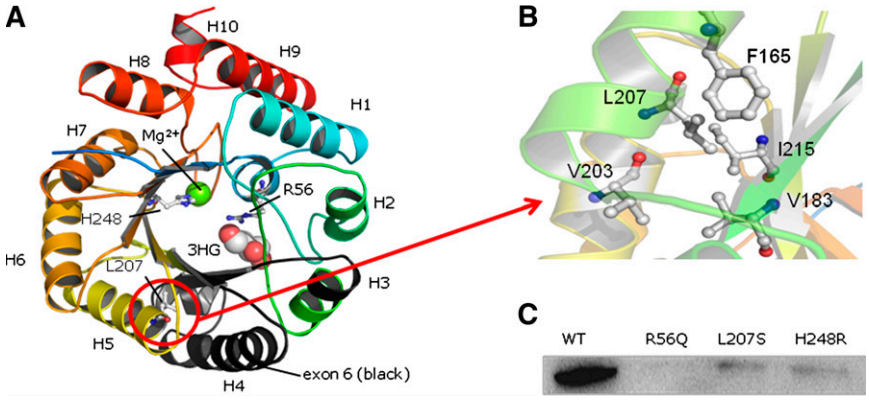

Fig. 1. 3D structure model for human er-cHL protein. (A) A 3D model of the protein core of human er-cHL protein. Secondary structure elements are included (H, helix; E, β sheet) and labeled according to their position in the template structure (H1 to H10; E1 to E8). The positions of the 3-hydroxy-glutaric acid (3HG) and Mg^{2+} ion in the modeled active center are labeled. The positions of mutated residues R56 and H248 in the active center and L207 in helix H5 are also indicated. Structure elements corresponding to exon 6 of er-cHL are shown in black. (B) Detailed zoom of hydrophobic residues in the neighborhood of L207. (C) Western blot of the human er-cHL protein (WT) and R56Q, L207S, and H248R mutants. Note that the WT protein is expressed in higher quantities than the mutant ones in the experimental system.

TABLE 1. Enzymatic activity of wild-type and mutants of human er-cHL protein

Protein	Enzymatic Activity (nmol × min^{-1} × mg^{-1})
er-cHL (WT)	25
L207S	ND
H248R	ND

ND, not detected.

blot using anti-er-cHL antibody. er-cHL was found in the cytosolic and ER fraction (**Fig. 2**). As controls, Western blot experiments were performed on the subcellular fractions using antibodies of known endoplasmic reticulum (calnexin) and cytosolic (β-actine) proteins (Fig. 2). As predicted, calnexin was detected in the ER membrane fraction but not in the cytosolic one; β-actine was detected only in the cytosolic fraction.

To further localize er-cHL protein, HEK293 cells were transiently transfected with *HMGCLL1*-pEGFP, which produces the 340 residues of the human protein, or with *HMGCL*-pDsRed2, which produces the 325 residues of the human protein. Seventy-two hours after transfection, the fluorescence pattern shown by *HMGCLL1*-pEGFP (which was expressed in a reticular manner) (**Fig. 3**, I–L) was different from that of *HMGCL*-pDsRed2 (which was expressed in a punctuate manner, like a mitochondrial pattern, as expected) (Fig. 3, A–D). In some experiments, cells were cotransfected with pDsRed2-ER (Clontech), a subcellular localization vector that stains the ER red. Fig. 3L shows that er-cHL is localized in the ER but not in mitochondria. To assess whether er-cHL is localized in peroxisomes, which are reported to have a pHL isoform (2), colocalization studies were performed with anti-PMP70, a peroxisomal membrane protein antibody (Fig. 3, E–H). No major colocalization was observed between PMP70 and er-cHL proteins. To check whether er-cHL is also located in cytosol, we labeled the cytosol of the cells with the anti-GAPDH antibody (Fig. 3, M–P). The results showed that the er-cHL is also located in the cytosol of HEK293 cells.

To confirm these results, we transfected HEK293 cells with the plasmid *HMGCLL1*-Tag3, performed the same proves, and obtained similar results (**Fig. 4**), which showed a cytosolic and ER distribution pattern.

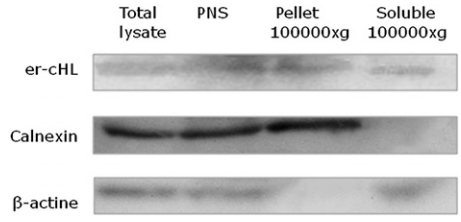

Fig. 2. Western blot of different subcellular fractions. Equal proportions of the fractions corresponded to the whole-cell lysate, postnuclear soluble fraction (PNS) and pellet, and supernatant from the 100,000 *g* centrifugation were immunoblotted and developed against er-cHL, calnexin, and β-actine proteins. The er-cHL protein is located in all the analyzed fractions. Calnexin is located in the whole-cell lysate, β-actine is located in the whole-cell lysate, and the PNS and the supernatant are from the 100,000 *g* centrifugation.

er-cHL can associate and dissociate from endoplasmic reticulum membranes. As described in Experimental Procedures, we treated the cloned and expressed er-cHL, the endoplasmic reticulum from adult human lung, and a mixture of both samples with Triton X-114. This reagent enabled us to separate the samples into two fractions, one soluble and the other insoluble. Then, Western blots of both fractions were performed.

The cloned er-cHL was a soluble protein (**Fig. 5A**). However, in the endoplasmic reticulum, we found the er-cHL in the membrane fraction (Fig. 5A). To determine whether the er-cHL could associate with the ER, we performed the same experiment with a mixture of the er-cHL protein and ER samples (Fig. 5A). The results suggest that cloned er-cHL protein can spontaneously associate with the endoplasmic reticulum membrane in vitro.

To find out whether er-cHL was an integral or peripheral membrane protein, we treated the ER membranes with $NaHCO_3$ 100 mM pH 11.5. The $NaHCO_3$ reagent causes the dissociation of the peripheral proteins because of their ionic strength. However, it cannot cause the solubilization of the membranes and separate the integral membrane proteins. Fig. 5B shows er-cHL in the membrane and the soluble fraction after treatment with $NaHCO_3$. This result showed that treatment with $NaHCO_3$ can cause dissociation of the endogenous er-cHL from the endoplasmic reticulum membrane. We performed the same experiment developing against calnexin, a known endoplasmic reticulum integral protein. The results showed that er-cHL and calnexin behaved differently following treatment with $NaHCO_3$. The treatment of the samples with Triton X-100 (1%) causes the dissociation of all the membrane proteins. The results showed that the er-cHL is only located in the soluble fraction after the treatment with Triton X-100, like the calnexin protein.

Kinetic analysis of enzyme er-cHL activity

The specific activity of each of the cloned er-cHL and mHL enzymes was determined using the enzymatically coupled spectrophotometric assay (27) (**Fig. 6**). As shown in **Table 2**, er-cHL activity was lower than mHL activity. The maximal V_{max} values were obtained at pH 8 for both enzymes. The Michaelis constant for the substrate, HMG-CoA, was determined for er-cHL and mHL (Table 2). In both cases, the measured values differ between pH 8 and 9.

We also determined the specific lyase activity and the Michaelis constant for the mitochondrial and cytosolic + reticulum fractions of the human testis tissue. The mitochondrial activity was higher than the cytosolic + reticulum (Table 2). The K_m value for the mitochondrial fraction does not vary much between pHs, and it is also higher than the cytosolic + reticulum K_m value. The $\Delta V_{max}/K_m$ relationships between the cloned er-cHL and mHL proteins and the subcellular fractions were similar.

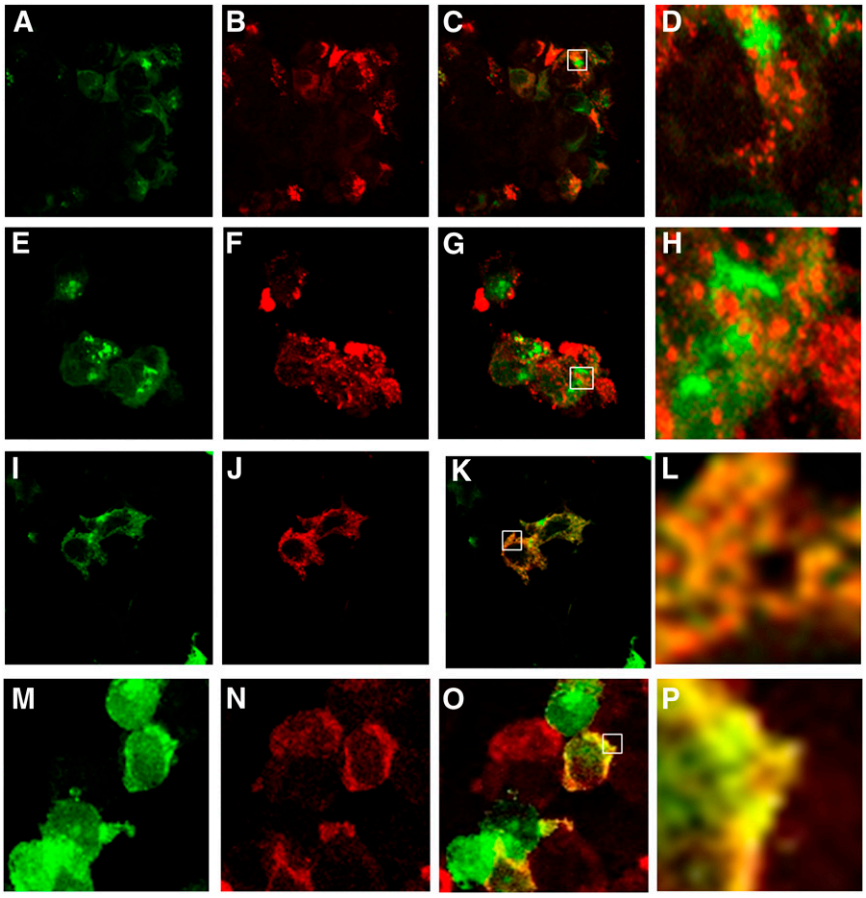

Fig. 3. Colocalization studies of er-cHL protein in cell cultures using the pEGFP plasmid. HEK293 cells were transfected with *HMGCLL1*-pEGFP (A–P) and then cotransfected with *HMGCL*-pDsRed2 (A–D), incubated with anti-PMP70 as the primary antibody (E–H), cotransfected with pDsRed2-ER (I–L), or incubated with anti-GAPDH (M–P). Images show that the er-cHL protein is colocalized with the endoplasmic reticulum (K and L) and the cytosol (O and P) but not with the mitochondria (C and D) or the peroxisomes (G and H). Images were taken by confocal microscopy with a filter to detect green emission, red emission, or the merged image (C, G, K, and o). Images D, H, L, and P are a higher magnification of the selected area from the C, G, K, and O images, respectively.

To find out whether the spliced variants of the er-cHL enzyme also had lyase activity, we carried out directed mutagenesis to remove exon 6. The results showed that the spliced protein had no lyase activity in a eukaryotic model.

Tissue distribution of er-cHL protein and tissue-specific lyase activity measures

We measured lyase activity in the cytosol + ER fraction of several tissues (liver, brain, pancreas, lung, kidney, and testis). We found lyase activity in all the tissues assayed. The maximum activity was found in lung, with a value of 52.14 nmol × min^{-1} × g^{-1} tissue, followed by kidney (33.18 nmol × min^{-1} × g^{-1} tissue), liver (19.55 nmol × min^{-1} × g^{-1} tissue), testis (18.42 nmol × min^{-1} × g^{-1} tissue), pancreas (17.84 nmol × min^{-1} × g^{-1} tissue), and brain (10.24 nmol × min^{-1} × g^{-1} tissue) (**Fig. 7A**). We measured lyase activity in the mitochondrial fraction of the same tissues to compare the two values. The maximum activity value was found in liver (133.12 nmol × min^{-1} × g^{-1} tissue), followed by pancreas (58.5 nmol × min^{-1} × g^{-1} tissue), kidney (46.94 nmol × min^{-1} × g^{-1} tissue), testis (19.04 nmol × min^{-1} × g^{-1} tissue), lung (18.98 nmol × min^{-1} × g^{-1} tissue), and brain (0 nmol × min^{-1} × g^{-1} tissue) (**Fig. 8**).

We performed Western blot experiments to measure the protein expression level in different human tissues. We used the endoplasmic reticulum of several tissues as a sample. The highest protein levels were found in human kidney, followed by lung, brain, liver, testis, and pancreas (Fig. 7B).

DISCUSSION

In this study, the occurrence of a novel extra mitochondrial HMG-CoA lyase, with a dual location in the endoplasmic reticulum and in the cytosol (er-cHL), is reported for first time. It is encoded by a different gene (*HMGCLL1*) to the mitochondrial HL or peroxisomal HL enzymes (*HMGCL*). The results outlined here allow us to accurately characterize the novel enzyme and provide clues about its functional role.

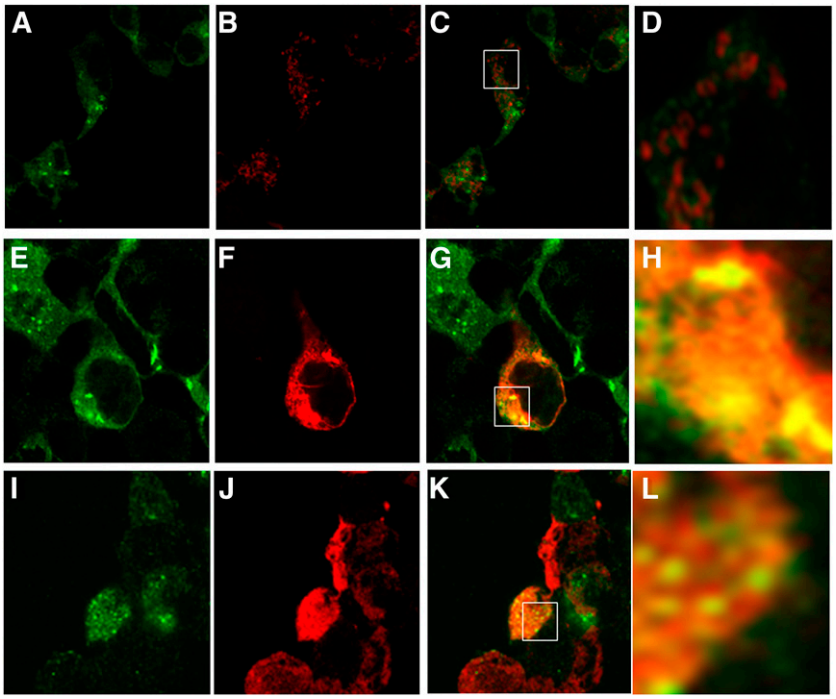

Fig. 4. Colocalization studies of er-cHL protein in cell cultures using the pTag3 plasmid. HEK293 cells were transfected with *HMGCLL1*-pTag3 (A–L) and cotransfected with *HMGCL*-pTag3 (A–D), cotransfected with pDsRed2-ER (E–H) or incubated with anti-GAPDH (I–L). Images showed that the er-cHL protein is colocalized with the endoplasmic reticulum (F and H) and the cytosol (K and L) but not with the mitochondria (C and D). Images were taken by confocal microscopy with a filter to detect green emission, red emission or the merged image (C, G, and K). Images D, H, and L are a higher magnification of the selected area from the C, G, and K images, respectively.

The novel *HMGCLL1* gene is reported in the National Center for Biotechnical Information and Ensembl. The comparative study of the *HMGCLL1* and *HMGCL* genes shows identities of 67% (mRNA) and 70% (protein) of the core sequence of the encoded protein. *HMGCLL1* is in the short arm of the chromosome 6, while the *HMGCL* gene is located in the short arm of chromosome 1. Although the *HGMCLL1* gene has 11 exons and 10 introns, no variant

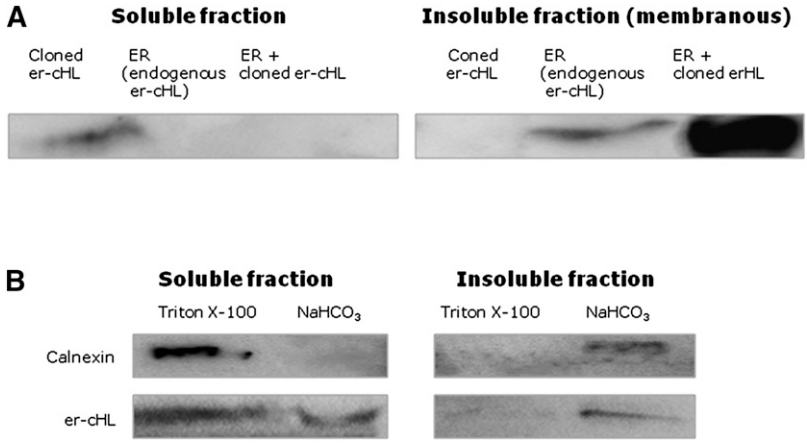

Fig. 5. Association and dissociation er-cHL experiments. (A) Association experiment. Western blot shows that the cloned er-cHL protein is soluble but not insoluble. The endogenous er-cHL protein is located in the ER membranes (insoluble fraction) but not in the soluble one. The mixture of ER membranes plus cloned er-cHL protein is located in the insoluble (membranous) fraction and suggests that the er-cHL protein can associate with the membranes spontaneously in vitro. (B) Dissociation experiment. Samples were treated with PBS+Triton X-100 (1%) (control with detergent) or $NaHCO_3$ (100 mM pH 11.5). Western blot showed that the er-cHL protein is distributed between the soluble and the insoluble fractions after the treatment with $NaHCO_3$ and that it is only present in the soluble fraction after the treatment with Triton X-100. The calnexin protein is located in the insoluble fraction after the treatment with $NaHCO_3$ and in the soluble fraction after the treatment with Triton X-100.

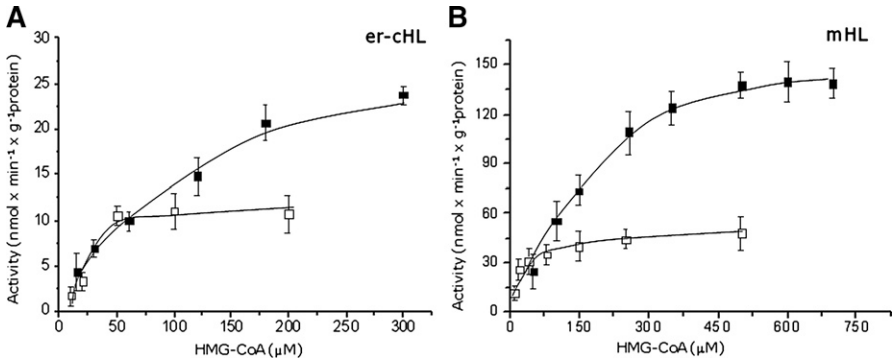

Fig. 6. Kinetic analysis of cloned er-cHL and mHL proteins. Black pH 8, white pH 9. Proteins were incubated at increasing concentrations of HMG-CoA and lyase activity was measured. (A) er-cHL protein. (B) mHL protein.

has been found to contain all the exons. The most frequent variant is called "variant b," which encodes 340 amino acids. This variant has a genomic organization similar to the *HMGCL* gene, with a high homology between 2 and 9 exons for the *HMGCL* gene, and 4 to 11 exons for the *HMGCLL1* gene (supplemental Fig. I). While the flanking exon sequences are similar in the two genes, the intron size is larger in the *HMGCLL1* gene. All these results suggest that these are paralogous genes (29) because they are highly homologous and occupy different sites within the same genome.

The *HMGCLL1* gene study shows a higher number of physiological splicing variants than those reported for the *HMGCL* gene (30, 31). If we take "variant b" as a reference, the alternative transcripts can be classified into two groups, according to exon insertion or deletion. "Variant a" has the insertion of exon 2, while "variant c" has the insertion of exon 3. Both have only been amplified in one or two fetal tissues using specific primers, which suggests a rather low presence. However, "variant a" combines all the elements required to translate an active protein, whereas "variant c" has a premature STOP codon and encodes a protein of 53 amino acids without a catalytic center.

All the deletion variants start with the skipping of the exon 2 or 6. This fact has been related with a drag mechanism of these exons over the rest, as proposed for other genes (31–35). Furthermore, all lack exon 6. To find out whether these variants are functional, the common exon 6 was deleted in the cloned whole protein. The loss of activity of the er-cHL-del6 suggests that none of the deleted forms has any activity. The presence of these inactive variants in tissues could be related with a block mechanism of the whole protein, as suggested for the mitochondrial HMG-CoA synthase and lyase (32).

The high 70% sequence identity between er-cHL and mHL led us to propose a 3D structural model for er-cHL (Fig. 1). Like mHL, the catalytic domain of er-cHL exhibits a TIM barrel $(\beta\alpha)_8$ structure, with two additional α helices (H9 and H10) located at the COOH end in contact with H1 and H8. The comparison between the amino acid sequence of the two proteins (supplemental Fig. III) indicates that all the motifs previously shown to be essential for lyase activity and substrate binding in the mHL enzyme (3, 4, 6–9) are completely conserved in er-cHL and so presumably located at equivalent positions in the active site of both enzymes. Mutations of p.L207S and p.H248R in er-cHL exhibit a complete lack of enzymatic activity, as described for the mHL mutants. This supports the accuracy of the proposed model for er-cHL.

The studies performed in cells culture to identify the subcellular localization of the er-cHL show that it is located in the endoplasmic reticulum and in the cytosol (Figs. 3 and 4) but not in mitochondria or peroxisomes, like the HL (2). Furthermore, the association-dissociation experiment shows us that the novel enzyme is located in the ER membranes but that it is not an integral membrane protein (Fig. 5). As Guo et al. (36) reported the presence of a β-hydroxybutyrate deshydrogenase, only an enzyme with lyase capacity was necessary to close the ketone body synthesis cytosolic pathway. The findings

TABLE 2. Kinetic constants from the cloned er-cHL and mHL proteins, and from the mitochondrial and cytosol + reticulum human testis fractions at different pHs

	pH	mHL	er-cHL	Mitochondria	Cytosol + Reticulum
V_{max} [a]	9	50 ± 4	12 ± 2	0.17 ± 0.02	0.027 ± 0.003
	8	145 ± 5	25 ± 1	0.08 ± 0.02	0.024 ± 0.004
K_m [b]	9	25 ± 2	40 ± 3	175 ± 5	190 ± 7
	8	140 ± 6	75 ± 4	200 ± 5	175 ± 4
$\Delta\ V_{max}/K_m$ [c]	8→9	0.52	1.10	0.41	0.96

[a] V_{max} expressed in nmol × min^{-1} × mg^{-1} protein.
[b] K_m expressed in μM.
[c] Δ calculated as a ratio of pH 8 to pH 9 values.

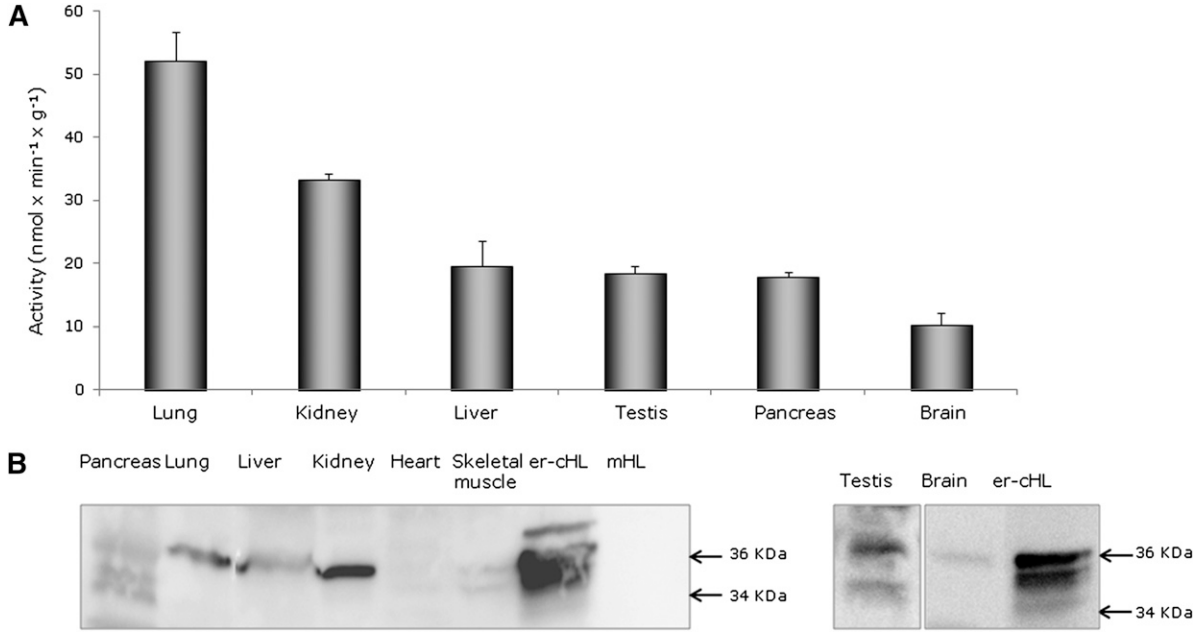

Fig. 7. Western blot and activity level of er-cHL in different human tissues. (A) er-cHL activity was measured in the cytosolic + endoplasmic reticulum fraction of human adult tissues spectrophotometrically. Data are presented as mean ± SEM (n = 4). Four tissue samples were measured, two from each subject. (B) Western blot for the endoplasmic reticulum fraction of different adult human tissues. Due to the proteolysis process, several Western blots were carried out to assess whether er-cHL protein was present in the different tissues. We show the positive here. Cloned er-cHL and mHL proteins are put as control of the antibody specificity.

of the er-cHL enzyme suggest at least the closure of this metabolic pathway.

The activity experiments show different kinetic parameters for the two isoenzymes (Table 2). Thus, er-cHL has a lower enzymatic rate and a higher substrate affinity than mHL, which suggests that it functions in a subcellular compartment where substrate availability may be low. Moreover, these results have been confirmed in different subcellular fractions of human testis. The kinetic characteristics of the cloned proteins and the subcellular fractions are similar. The data obtained for the er-cHL are similar to those found in the cytosol + reticulum fraction and for mHL and the mitochondrial fraction. All of these results reinforce the idea that these are the subcellular compartments in which both enzymes function.

The activity and expression tissue level results for er-cHL show a characteristic and different distribution pattern than the mHL (11) (Fig. 8). The absence of mHL activity in brain (11) contrasts with appreciable er-cHL activity in this tissue, and it was initially suggested that these could be two tissue-specific isoenzymes. However, the high mHL activity in liver, the main ketogenic organ, is not accompanied by an absence of activity of the novel enzyme. The liver may also need the ketone bodies in normal-glycemic states, when the mHL is inactive. In these conditions, the er-cHL enzyme could play its functional role.

The results obtained in lung support a similar idea. In this organ, the synthesis of alveolar surfactant depends on the availability of glucose and ketone bodies (37, 38). The high novel enzyme activity in this tissue could be related with this synthesis. This hypothesis is supported by the absence of respiratory pathology in patients with 3-hydroxy-3-methylglutaric aciduria. In acute crisis, these patients develop a hypoglycemic hypoketonemic profile (1), in which the main substrates for surfactant synthesis are absent. However, this condition does not alter respiratory activity, perhaps because the er-cHL can produce the required ketone bodies in situ in the cytosol.

The finding of er-cHL in brain suggests that the novel enzyme could play a key role in this tissue. Ketone bodies in brain are an alternative energy source to glucose (39). Moreover, they have other functions, such as supplying the substrate for myelin lipid synthesis (40) and neuroprotection

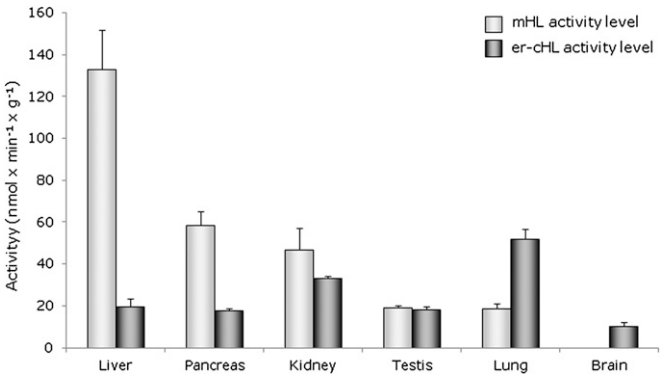

Fig. 8. Activity level comparison of er-cHL and mHL protein in different adult human tissues. The measured activity level of the endoplasmic reticulum + cytosolic (er-cHL) and mitochondria (mHL) fraction is shown. The mHL activity level is higher than that of er-cHL in most of the assayed tissues, except in lung and brain where er-cHL activity is high. White bars corresponded to mHL activity, and black bars corresponded to er-cHL activity.

(41–43). If cerebral ketone bodies depend exclusively on hepatic mHL activity, they can only be used in hypoglycemic situations. However, neuroprotective functions are not limited to this metabolic state. The er-cHL of the brain could provide the ketone bodies required to carry out these roles in situ in the cytosol. Furthermore, there is controversy as to whether there is brain lyase activity (26, 44–46). The finding of lyase activity in the cytosol + endoplasmic reticulum fraction (er-cHL) and its absence in the mitochondrial fraction (mHL) (11) could resolve this issue.

In summary, with the finding of the er-cHL in the cytosolic and endoplasmic reticulum, the ketone body synthesis pathway in cytosol is completed. To date, the presence of this pathway had only been demonstrated in mitochondria or peroxisomes. Moreover, the tissue distribution pattern of the novel isoenzyme suggests that er-cHL and mHL perform different actions. While the mHL has a clear energy metabolism role, the er-cHL could be involved in other metabolic functions.

The authors thank Rebeca Escosa Vela, who provided technical support, and Robin Rycroft. who provided editorial help.

REFERENCES

1. Faull, K. F., P. D. Bolton, B. Halpern, J. Hammond, and D. M. Danks. 1976. The urinary organic acid profile associated with 3-hydroxy-3-methylglutaric aciduria. *Clin. Chim. Acta.* **73:** 553–559.
2. Ashmarina, L. I., N. Rusnak, H. M. Miziorko, and G. A. Mitchell. 1994. 3-Hydroxy-3-methylglutaryl-CoA lyase is present in mouse and human liver peroxisomes. *J. Biol. Chem.* **269:** 31929–31932.
3. Fu, Z., J. A. Runquist, F. Forouhar, M. Hussain, J. F. Hunt, H. M. Miziorko, and J. J. Kim. 2006. Crystal structure of human 3-hydroxy-3-methylglutaryl-CoA Lyase: insights into catalysis and the molecular basis for hydroxymethylglutaric aciduria. *J. Biol. Chem.* **281:** 7526–7532.
4. Fu, Z., J. A. Runquist, C. Montgomery, H. M. Miziorko, and J. J. Kim. 2010. Functional insights into human HMG-CoA lyase from structures of Acyl-CoA-containing ternary complexes. *J. Biol. Chem.* **285:** 26341–26349.
5. Kramer, P. R., and H. M. Miziorko. 1980. Purification and characterization of avian liver 3-hydroxy-3-methylglutaryl coenzyme A lyase. *J. Biol. Chem.* **255:** 11023–11028.
6. Montgomery, C., and H. M. Miziorko. 2011. Influence of multiple cysteines on human 3-hydroxy-3-methylglutaryl-CoA lyase activity and formation of inter-subunit adducts. *Arch. Biochem. Biophys.* **511:** 48–55.
7. Roberts, J. R., C. Narasimhan, and H. M. Miziorko. 1995. Evaluation of cysteine 266 of human 3-hydroxy-3-methylglutaryl-CoA lyase as a catalytic residue. *J. Biol. Chem.* **270:** 17311–17316.
8. Roberts, J. R., G. A. Mitchell, and H. M. Miziorko. 1996. Modeling of a mutation responsible for human 3-hydroxy-3-methylglutaryl-CoA lyase deficiency implicates histidine 233 as an active site residue. *J. Biol. Chem.* **271:** 24604–24609.
9. Tuinstra, R. L., and H. M. Miziorko. 2003. Investigation of conserved acidic residues in 3-hydroxy-3-methylglutaryl-CoA lyase: implications for human disease and for functional roles in a family of related proteins. *J. Biol. Chem.* **278:** 37092–37098.
10. Casals, N., P. Gómez-Puertas, J. Pié, C. Mir, R. Roca, B. Puisac, R. Aledo, J. Clotet, S. Menao, D. Serra, et al. 2003. Structural (betaalpha)8 TIM barrel model of 3-hydroxy-3-methylglutaryl-coenzyme A lyase. *J. Biol. Chem.* **278:** 29016–29023.
11. Puisac, B., M. Arnedo, C. H. Casale, M. P. Ribate, T. Castiella, F. J. Ramos, A. Ribes, C. Pérez-Cerdá, N. Casals, F. G. Hegardt, et al. 2010. Differential HMG-CoA lyase expression in human tissues provides clues about 3-hydroxy-3-methylglutaric aciduria. *J. Inherit. Metab. Dis.* **33:** 405–410.
12. Pié, J., N. Casals, B. Puisac, and F. G. Hegardt. 2003. Molecular basis of 3-hydroxy-3-methylglutaric aciduria. *J. Physiol. Biochem.* **59:** 311–321.
13. Pié, J., E. López-Viñas, B. Puisac, S. Menao, A. Pié, C. Casale, F. J. Ramos, F. G. Hegardt, P. Gómez-Puertas, and N. Casals. 2007. Molecular genetics of HMG-CoA lyase deficiency. *Mol. Genet. Metab.* **92:** 198–209.
14. Krisans, S. K. 1996. Cell compartmentalization of cholesterol biosynthesis. *Ann. N. Y. Acad. Sci.* **804:** 142–164.
15. Ashmarina, L. I., M. F. Robert, M. A. Elsliger, and G. A. Mitchell. 1996. Characterization of the hydroxymethylglutaryl-CoA lyase precursor, a protein targeted to peroxisomes and mitochondria. *Biochem. J.* **315:** 71–75.
16. Tuinstra, R. L., J. W. Burgner 2nd, and H. M. Miziorko. 2002. Investigation of the oligomeric status of the peroxisomal isoform of human 3-hydroxy-3-methylglutaryl-CoA lyase. *Arch. Biochem. Biophys.* **408:** 286–294.
17. Guex, N., A. Diemand, and M. C. Peitsch. 1999. Protein modelling for all. *Trends Biochem. Sci.* **24:** 364–367.
18. Peitsch, M. C. 1996. ProMod and Swiss-Model: internet-based tools for automated comparative protein modelling. *Biochem. Soc. Trans.* **24:** 274–279.
19. Schwede, T., J. Kopp, N. Guex, and M. C. Peitsch. 2003. SWISS-MODEL: an automated protein homology-modeling server. *Nucleic Acids Res.* **31:** 3381–3385.
20. Benkert, P., M. Biasini, and T. Schewede. 2011. Toward the estimation of the absolute quality of individual protein structure models. *Bioinformatics.* **27:** 343–350.
21. Guex, N., and M. C. Peitsch. 1997. SWISS-MODEL and the Swiss-PdbViewer: an environment for comparative protein modeling. *Electrophoresis.* **18:** 2714–2723.
22. Menao, S., E. López-Viñas, C. Mir, B. Puisac, E. Gratacós, M. Arnedo, P. Carrasco, S. Moreno, M. Ramos, M. C. Gil, et al. 2009. Ten novel HMGCL mutations in 24 patients of different origin with 3-hydroxy-3-methyl-glutaric aciduria. *Hum. Mutat.* **30:** E520–E529.
23. Casale, C. H., A. D. Alonso, and H. S. Barra. 2001. Brain plasma membrane Na+,K+-ATPase is inhibited by acetylated tubulin. *Mol. Cell. Biochem.* **216:** 85–92.
24. Callan, A. C., S. Bunning, O. T. Jones, S. High, and E. Swanton. 2007. Biosynthesis of the dystonia-associated AAA+ ATPase torsinA at the endoplasmic reticulum. *Biochem. J.* **401:** 607–612.
25. Clinkenbeard, K. D., W. D. Reed, R. A. Mooney, and M. D. Lane. 1975. Intracellular localization of the 3-hydroxy-3-methylglutaryl coenzme A cycle enzymes in liver. Separate cytoplasmic and mitochondrial 3-hydroxy-3-methylglutaryl coenzyme A generating systems for cholesterogenesis and ketogenesis. *J. Biol. Chem.* **250:** 3108–3116.
26. Wanders, R. J., R. B. Shutgens, and P. H. Zoeters. 1988. 3-Hydroxy-3-methylglutaryl-CoA lyase in human skin fibroblasts: study of its properties and deficient activity in 3-hydroxy-3-methylglutaric aciduria patients using a simple spectrophotometric method. *Clin. Chim. Acta.* **171:** 95–101.
27. Mitchell, G. A., P. T. Ozand, M. F. Robert, L. Ashmarina, J. Roberts, K. M. Gibson, R. J. Wanders, S. Wang, I. Chevalier, E. Plöchl, et al. 1998. HMG CoA lyase deficiency: identification of five causal point mutations in codons 41 and 42, including a frequent Saudi Arabian mutation, R41Q. *Am. J. Hum. Genet.* **62:** 295–300.
28. Ozand, P. T., A. al Aqeel, G. Gascon, J. Brismar, E. Thomas, and H. Gleispach. 1991. 3-Hydroxy-3-methylglutaryl-coenzyme A (HMG-CoA) lyase deficiency in Saudi Arabia. *J. Inherit. Metab. Dis.* **14:** 174–188.
29. Strachan, T. 1992. The Human Genome. Bios Scientific Publishers, Oxford.
30. Muroi, J., T. Yorifuji, A. Uematsu, Y. Shigematsu, K. Onigata, H. Maruyama, T. Nobutoki, A. Kitamura, and T. Nakahata. 2000. Molecular and clinical analysis of Japanese patients with 3-hydroxy-3-methylglutaryl CoA lyase (HL) deficiency. *Hum. Genet.* **107:** 320–326.
31. Puisac, B., M. Ramos, M. Arnedo, S. Menao, M. C. Gil-Rodríguez, M. E. Teresa-Rodrigo, A. Pié, J. C. de Karam, J. J. Wesselink, I. Giménez, et al. 2012. Characterization of splice variants of the genes encoding human mitochondrial HMG-CoA lyase and HMG-CoA synthase, the main enzymes of the ketogenesis pathway. *Mol. Biol. Rep.* **39:** 4777–4785.
32. Li, J., Y. Sheng, P. Z. Tang, C. H. Tsai-Morris, and M. L. Dufau. 2006. Tissue-cell- and species-specific expression of gonadotropinregulated

long chain acyl-CoA synthetase (GR-LACS) in gonads, adrenal and brain. Identification of novel forms in the brain. *J. Steroid Biochem. Mol. Biol.* **98:** 207–217.
33. Rickers, A., F. Rininsland, L. Osborne, and J. Reiss. 1994. Skipping of multiple CFTR exons is not a result of single exon omissions. *Hum. Genet.* **94:** 311–313.
34. Casale, C. H., N. Casals, J. Pié, N. Zapater, C. Pérez-Cerdá, B. Merinero, M. Martínez-Pardo, J. J. García-Peñas, J. M. García-Gonzalez, R. Lama, et al. 1998. A nonsense mutation in the exon 2 of the 3-hydroxy-3-methylglutaryl coenzyme A lyase (HL) gene producing three mature mRNAs is the main cause of 3-hydroxy-3-methylglutaric aciduria in European Mediterranean patients. *Arch. Biochem. Biophys.* **349:** 129–137.
35. Valentine, C. R. 1998. The association of nonsense codons with exon skipping. *Mutat. Res.* **411:** 87–117.
36. Guo, K., P. Lukacik, E. Papagrigoriou, M. Meier, W. H. Lee, J. Adanski, and U. Oppermann. 2006. Characterization of human DHRS6, an orphan short chain dehydrogenase/reductase enzyme: a novel, cytosolic type 2 R-beta-hydroxybutyrate dehydrogenase. *J. Biol. Chem.* **281:** 10291–10297.
37. Harwood, H. J., Jr., M. Schneider, and P. W. Stacpoole. 1984. Measurement of human leukocyte microsomal HMG-CoA reductase activity. *J. Lipid Res.* **25:** 967–978.
38. Fox, R. E., I. B. Hopkins, E. T. Cabacungan, and J. T. Tildon. 1996. The role of glutamine and other alternate substrates as energy sources in the fetal rat lung type II cell. *Pediatr. Res.* **40:** 135–141.
39. Morris, A. A. 2005. Cerebral ketone body metabolism. *J. Inherit. Metab. Dis.* **28:** 109–121.
40. Lopes-Cardozo, M., J. W. Koper, W. Klein, and L. M. Van Golde. 1984. Acetoacetate is a cholesterogenic precursor for myelinating rat brain and spinal cord. Incorporation of label from [3–14C] acetoacetate, [14C]glucose and 3H2O. *Biochim. Biophys. Acta.* **794:** 350–352.
41. Guzmán, M., and C. Blázquez. 2004. Ketone body synthesis in the brain: possible neuroprotective effects. *Prostaglandins Leukot. Essent. Fatty Acids.* **70:** 287–292.
42. Maalouf, M., P. G. Sullivan, L. Davis, D. Y. Kim, and J. M. Rho. 2007. Ketones inhibit mitochondrial production of reactive oxygen species production following glutamate excitotoxicity by increasing NADH oxidation. *Neuroscience.* **145:** 256–264.
43. Maalouf, M., J. M. Rho, and M. P. Mattson. 2009. The neuroprotective properties of calorie restriction, the ketogenic diet, and ketone bodies. *Brain Res. Rev.* **59:** 293–315.
44. Bachhawat, B. K., W. G. Robinson, and M. J. Coon. 1955. The enzymatic cleavage of beta-hydroxy-beta-methylglutaryl coenzyme A to acetoacetate and acetyl coenzyme A. *J. Biol. Chem.* **216:** 727–736.
45. McGarry, J. D., and D. W. Foster. 1969. Ketogenesis and cholesterol synthesis in normal and neoplastic tissues of the rat. *J. Biol. Chem.* **244:** 4251–4256.
46. Shah, S. N. 1982. Cytosolic 3-hydroxy-3-methyl glutaryl coenzyme a synthase in rat brain: properties and developmental change. *Neurochem. Res.* **7:** 1359–1366.